Proceedings of Global Power and Propulsion Society
ISSN-Nr: 2504-4400
GPPS Hong Kong 2023
October 17-19, 2023
www.gpps.global

GPPS-TC-2023-0132

An Efficient Multi-Fidelity Simulation Approach for Performance Prediction of Adaptive Cycle Engines

Wangzhi Zou
Tsinghua University
zwz20@mails.tsinghua.edu.cn
Beijing, China

Zhaoyun Song
Tsinghua University
szylast@mail.tsinghua.edu.cn
Beijing, China

Baotong Wang
Tsinghua University
wangbaotong@tsinghua.edu.cn
Beijing, China

Mengyang Wen
Tsinghua University
wmy20@mails.tsinghua.edu.cn
Beijing, China

Xinqian Zheng
Tsinghua University
zhengxq@tsinghua.edu.cn
Beijing, China

ABSTRACT

Adaptive cycle engine (ACE) with multi-stream, modulated bypass ratio, and high-thrust/high-efficiency mode provides the capability of multiple mission adaptation for the next-generation aviation propulsion system. The low-fidelity zero-dimensional (0D) performance simulation method is commonly adopted in conventional engines such as turbofan and turbojet. However, it is hard to accommodate well to ACE with complex variable geometry schemes and strong interaction between components. This paper presents an efficient multi-fidelity simulation approach, often referred to as component zooming, for predicting the performance of ACE with the three-stream configuration. The one-dimensional (1D) mean-line models of the adaptive fan and low-pressure turbine (LPT) are integrated into the 0D ACE model by the iteratively-coupled method. The performance predicted by the multi-fidelity ACE models with different component zooming strategies is compared. The maximum deviations of thrust, specific fuel consumption, turbine inlet temperature, and bypass ratio between the 0D/1D Adaptive Fan/1D LPT coupled model and 0D ACE model are -10.8%, -4.4%, -5.4% (-75K), and 1.6%, respectively, which are considerable and non-negligible for the application in the design stage of ACE. The computing time of all the multi-fidelity models is less than 2 minutes. The effects of the key aerodynamic parameters of the adaptive fan and LPT on the engine performance are also evaluated. The proposed approach provides a generic and efficient solution for multi-fidelity ACE performance prediction with acceptable computing resource requirements and time cost, which is applicable in the engine conceptual and preliminary design stage.

INTRODUCTION

Aero-engine design is always a process to compromise between multiple design targets. Commercial engines are often designed to achieve excellent fuel economy with compromised thrust performance, while military engines are primarily designed to provide superior thrust performance, even sacrificing the fuel economy. The design philosophy of the adaptive cycle engine (ACE) is to eliminate this traditional compromise process with multiple operating modes by introducing wide-range variable geometry mechanisms, which is considered a competitive candidate for the next-generation aviation propulsion system.

The development of ACE dates back to the 1960s, and at that time, it was known as the variable cycle engine (Johnson, 1995). After entering the 21st century, the concept of ACE was proposed in the Adaptive Versatile Engine Technology (ADVENT) program launched by the US. According to the definition of ACE by General Electric (GE Aerospace, 2023), ACE is an engine capable of providing the high-thrust mode for maximizing the power and high-efficiency mode to extend mission range, transforming mission capability and enabling unrestricted operations by automatically alternating between these modes dramatically. Compared with the earlier variable cycle engine, the key feature of ACE is the addition of the third air stream, which provides an extra source of cooling air to improve the propulsive and fuel efficiency, and most importantly, it enables a step-change in power and thermal management capability (Guy, 2021; GE Aerospace, 2023).

The operating modes, control schemes, and aerodynamic interaction between components of ACE are more complex than those of conventional turbofan and turbojet engines, which brings great challenges to ACE performance prediction. The low-fidelity 0D simulation method based on the generic characteristic maps of components is commonly adopted in the performance prediction of conventional engines. However, when applied to ACE, it is usually difficult to meet the design and analysis requirements of the engineers and researchers. Therefore, the multi-fidelity simulation method, often referred to as component zooming, is regarded as a promising tool for ACE performance prediction by coupling the high-fidelity component model with the 0D engine model to reach a good balance of computing time and accuracy.

Multi-fidelity simulation methods were proposed in Numerical Propulsion System Simulation (NPSS) program launched by the US (Claus et al., 1991) and Value Improvement through a Virtual Aeronautical Collaborative Enterprise (VIVACE) launched by the EU (Alexiou et al., 2007). Depending on the coupling tightness level, these methods can be classified as de-coupled, iteratively-coupled, and fully-coupled methods. Different methods have been applied to conventional engines (Alexiou et al., 2007; Pilet et al., 2011; Kim et al., 2015; Klein et al., 2017; Kolias et al., 2018;). Recently, these methods have been gradually used for ACE design or performance analysis, including coupling the high-fidelity models of variable area bypass injector (VABI) (Fu et al., 2021), nozzle (Connolly et al., 2014), and core-driven fan stage (CDFS) (Xiaobo et al., 2023) with the 0D ACE model. However, there are fewer studies on integrating the high-fidelity models of other critical components, such as the adaptive fan and variable geometry turbine, into the 0D ACE model.

A notable difference between the ACE and the conventional turbofan engine is the difference in the operating characteristics of the components on the low-pressure spool. In the ACE, the front end on the low-pressure spool is the adaptive fan with multi-stream, and the rear end is the variable geometry low-pressure turbine (LPT). The adaptive fan works to realize the functions such as flow rate adjustment, bypass ratio modulation, and thermal management. The LPT operates to achieve the optimal power distribution between the two spools and contributes to the operating mode switching, both of which are highly coupled with other components in the ACE. Nevertheless, the components on the high-pressure spool, including the high-pressure compressor (HPC) and the high-pressure turbine (HPT), generally operate more similarly to those in the conventional turbofan engine, with the former adopting the variable geometry design and the latter adopting the fixed geometry design.

In this paper, an ACE with a three-stream configuration is selected for the study. First, a 0D ACE model is established in Matlab and Simulink platform. Second, considering that the main operating difference between ACE and conventional engine exists in the low-pressure spool components as mentioned above, the 1D adaptive fan model and the 1D LPT model are built from the validated 1D mean-line analysis method of the fan and turbine, respectively. Then, the 1D adaptive fan model, the 1D LPT model, and the 0D ACE model are coupled for the multi-fidelity ACE performance analysis. Finally, the results of different multi-fidelity models and 0D model are compared in terms of the engine performance and computing time, and the effects of the key aerodynamic parameters on the engine performance are evaluated.

METHODOLOGY

0D ACE Performance Simulation

The 0-D ACE performance model is developed in Matlab and Simulink platform based on object-oriented programming technology, using the open-source package T-MATS (Toolbox for the Modeling and Analysis of Thermodynamic Systems) released by NASA Glenn Research Center (Chapman et al., 2014). Because no engine test data is available to validate the established model in this paper, the trust in the model accuracy is placed on the soundness of the developed modeling methodologies and the results, which showed expected trends for the most part (Kopasakis et al., 2015). For the above purposes, two validation cases are presented to demonstrate the accuracy of the 0D performance modeling methodologies. The first case is the performance comparison between the test and T-MATS data for a mixed-flow turbofan engine, as shown in Figure 1. All the parameters are normalized by the corresponding test value at 100% design speed. In the modeling, the performance maps of the fan, HPC, HPT, and LPT were obtained from the component tests. It is found that the performance deviations between the test data and T-MATS data are less than 2%, and the trends of all the performance changes with the low-pressure spool speed predicted by T-MATS agree well with those of the test. Although the ACE and the mixed-flow turbofan engine are different in configuration, the results indicate the reliability of the modeling methodologies on the multi-stream engine to some extent. The second case is the performance comparison between the commercial software GasTurb and T-MATS for the F120 double-bypass variable cycle engine. As shown in Figure 2, the key performance parameters, including thrust, fuel mass flow, turbine inlet temperature (T4), and bypass ratio, as well as the operating lines predicted by T-MATS, agree well with those of GasTurb, except for the large thrust deviation at the low rotational speed caused by the different mixer modeling method, which proves the validity of the modeling methodologies.

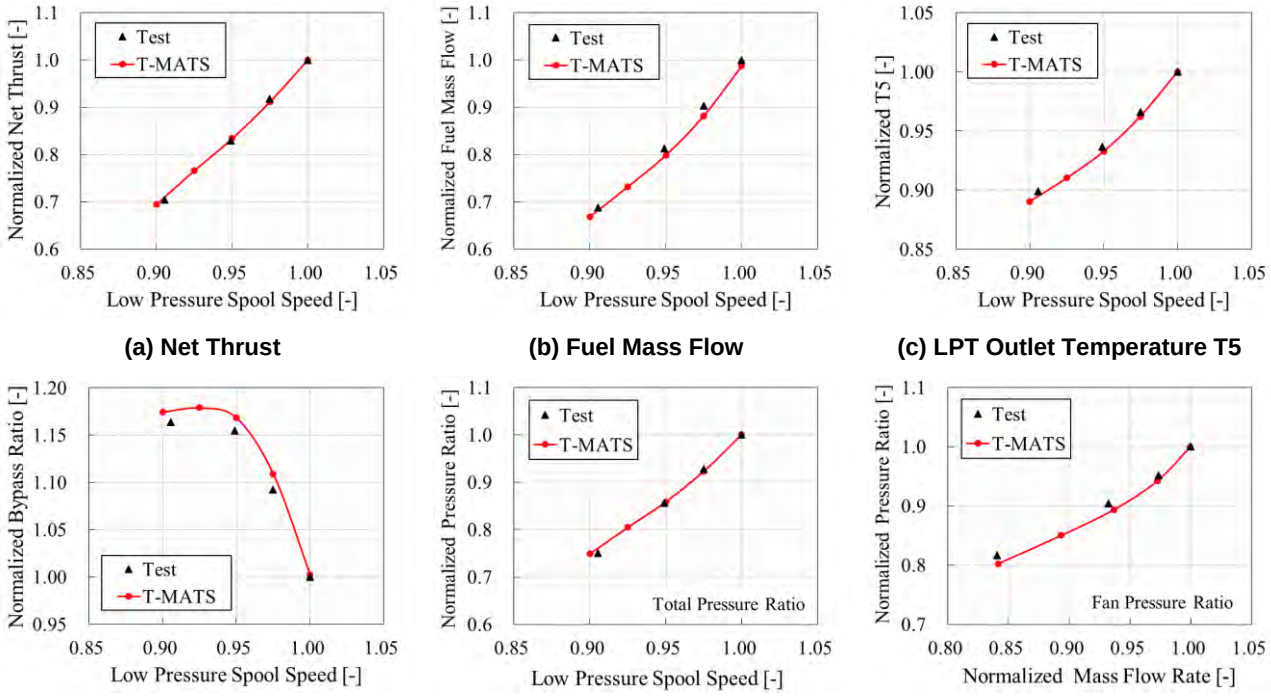

(a) Net Thrust (b) Fuel Mass Flow (c) LPT Outlet Temperature T5

(d) Bypass Ratio (e) Total Pressure Ratio (f) Operating Line on Fan Map

Figure 1 Mixed-Flow Turbofan Engine Performance Comparison between Test and T-MATS

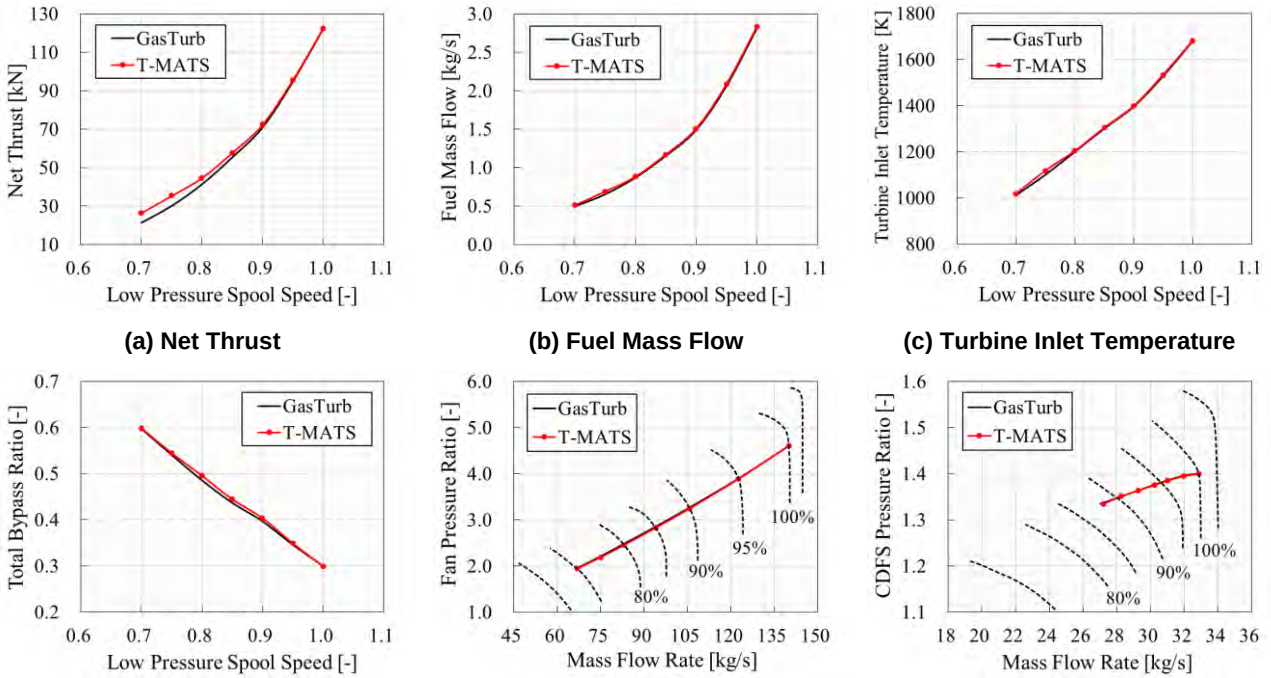

(a) Net Thrust (b) Fuel Mass Flow (c) Turbine Inlet Temperature

(d) Total Bypass Ratio (e) Operating Line on Fan Map (f) Operating Line on CDFS Map

Figure 2 F120 Performance Comparison between GasTurb and T-MATS

The modulating bypass (MOBY) variable cycle engine configuration was proposed by General Electric in the 1970s (Johnson, 1995), as shown in Figure 3, which laid an important foundation for the development of variable cycle engines and ACEs. The MOBY consists of three spools, two-section split fans, the duct burner, and three variable separated flow nozzles, which are highly complex in structure. In this paper, an ACE with a three-stream configuration is selected for study, and the schematic diagram is shown in Figure 4. Compared with MOBY, the three-spool configuration is replaced by the two-spool configuration, the two-section split fans are on one spool, and the duct burner is removed in this ACE. The ACE consists of the adaptive fan which includes the front fan and the rear fan, the HPC, the combustor, the HPT, the

LPT, the core nozzle, the first bypass nozzle, and the second bypass nozzle. The guide vane or stator vane angle of the front fan, rear fan, HPC, HPT, LPT, and the throat areas of three nozzles are adjustable, as shown in Figure 4. To represent the effects of variable geometry on the component characteristics, multi-angle characteristic maps (Sullivan and Parker, 1979), which contain information on the mass flow rate, pressure ratio, and isentropic efficiency under different guide vane angles, are used for the front fan and rear fan, and the empirical relations (Edmunds, 1977; Grönstedt, 2000) to predict the maps with changed guide vane or stator vane angle are used for the HPC, HPT, and LPT.

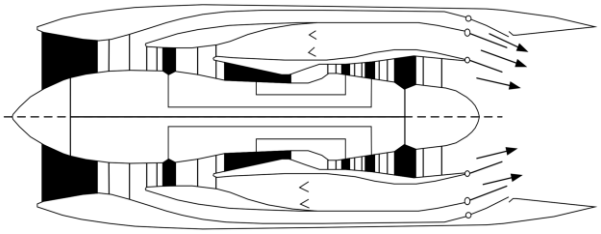

Figure 3 Three-Spool Double Bypass MOBY

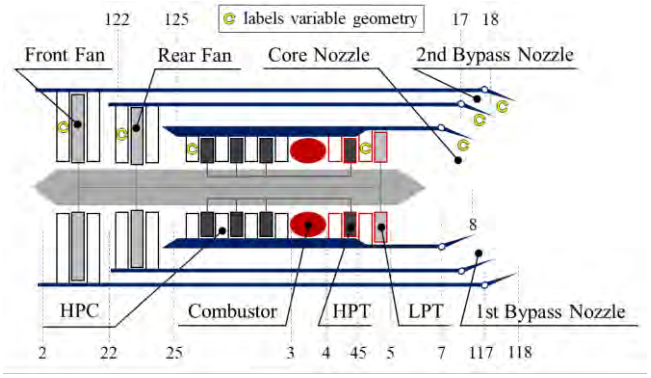

Figure 4 Three-Stream ACE Configuration

The design point of ACE is selected at sea level and static state, and the main parameters at the design point are shown in Table 1. The front fan split ratio is equal to the ratio of the mass flow rate in the second bypass duct to the mass flow rate in the rear fan. The rear fan split ratio is equal to the ratio of the mass flow rate in the first bypass duct to the mass flow rate in the HPC. The iteration and error variables of ACE to reach the convergence of equations based on the matching of each component at the off-design point are shown in Table 2. The low-pressure spool speed is set, and the Newton-Raphson iterative method is adopted to calculate the off-design point performance.

Table 1 Design Point Parameters

Parameter	Value	Unit
Front fan pressure ratio	2.1	-
Rear fan pressure ratio	1.45	-
HPC pressure ratio	6.0	-
T4	1700	K
Front fan bypass ratio	0.3	-
Rear fan bypass ratio	1.0	-
Specific thrust	501.5	m/s
SFC	66.52	kg/(kN·h)

Table 2 Off-Design Point Iteration and Error Variables

Component Class	Class number	Iteration variable	Error variable
Inlet	1	Mass flow	-
Compressor	3	R-value	Mass flow
Splitter	2	Split ratio	-
Burner	1	Fuel air ratio	-
Turbine	2	Expansion ratio	Mass flow
Nozzle	3	-	Mass flow
Shaft	2	Spool speed	Power
Summary	**14**	**11**	**10**

1D Adaptive Fan and 1D LPT Mean-Line Analysis

The turbomachinery 1D mean-line analysis approach plays an essential role in the engine conceptual and preliminary design stage due to its simplicity and rapidity. Compared with the scaled generic characteristic maps in the 0D ACE model, the characteristics from the 1D mean-line analysis are usually with higher accuracy and fidelity, because it is a physics-based approach. The effects of the variable guide vane/stator vane, tip clearance, and other second-order effects on the engine performance can be taken into account in detail.

The accuracy of the 1D mean-line analysis mainly depends on the loss and deviation models. Many empirical correlations for the loss and deviation models have been proposed by researchers in turbomachinery, based on a great amount of cascade test data. However, these models are commonly suitable for the early standard blade profiles and can obtain good performance prediction accuracy in the low-speed turbomachinery. On the other hand, with the development of turbomachinery design technology, advanced three-dimensional blade profiles have been widely used in high-performance turbomachinery. Therefore, the early proposed model coefficients need to be updated to meet the performance prediction requirements with the changed turbomachinery design strategy.

The 1D adaptive fan and 1D LPT mean-line analysis approach adopted in this paper are developed in the literature (Zhaoyun et al., 2022) and (Baotong et al., 2022), respectively. In both literatures, the empirical coefficients of the loss and deviation models are optimized based on the performance test results of multiple cases. The genetic algorithm is adopted for optimizing the empirical coefficients in the loss and deviation models. Hausdorff distance is employed for quantifying the discrepancy between the test and 1D prediction performance, which is taken as the optimization objective function. The optimized profile loss model and deviation model are briefly described below.

In the 1D adaptive fan mean-line analysis approach, the off-design profile loss model is shown in Equation (1), and the deviation model is shown in Equation (2). The empirical coefficients of both models are optimized from the Creveling model (Creveling and Carmody, 1967). In Equation (1), ω, i, and M_{in} denote the profile loss coefficient, incidence angle, and inlet Mach number, respectively. The subscript ref denotes the parameters in the reference state. In Equation (2), δ denotes the deviation angle, ε denotes the flow turning angle, and x is a function of i, i_{ref}, and ε.

$$\omega = \begin{cases} \omega_{\text{ref}} + 0.0005\left(i - i_{\text{ref}}\right)^2 & M_{in} < 0.6 \\ \omega_{\text{ref}} + \left(-0.0053 + 0.011 M_{\text{in}}\right)\left(i - i_{\text{ref}}\right)^2 & 0.6 \le M_{in} \le 0.95 \\ \omega_{\text{ref}} + \left(-0.0594 + 0.073 M_{\text{in}}\right)\left(i - i_{\text{ref}}\right)^2 & M_{in} > 0.95 \end{cases} \tag{1}$$

$$\delta = \begin{cases} \delta_{\text{ref}} + \left(-0.0247 + 0.4696x - x^2\right)\varepsilon & x \ge 0 \\ \delta_{\text{ref}} + \left(0.0655 + 0.3941x + 0.2572x^2\right)\varepsilon & x < 0 \end{cases} \tag{2}$$

In the 1D LPT mean-line analysis approach, the off-design profile loss model is shown in Equation (3), the empirical coefficients of which are optimized based on the Kacker and Okapuu model (Kacker and Okapuu, 1982), and the deviation model is shown in Equation (4), the empirical coefficients of which is optimized from the Zhu and Sjolander model (Junqiang and Sjolander, 2005). In Equation (3), i_{stall} means the stalling incidence angle. In Equation (4), γ, c, β_1, $\beta_{1\text{m}}$, $\beta_{2\text{m}}$, $t_{\max}$, Re denote the stagger angle, chord length, inlet flow angle, inlet metal angle, outlet metal angle, maximum blade thickness, and Reynolds number, respectively.

$$\omega = \left[0.2235\left(i/i_{\text{stall}}\right)^3 + 1.4057\left(i/i_{\text{stall}}\right)^2 + 0.4796\left(i/i_{\text{stall}}\right) + 1.0\right]\omega_{\text{ref}} \tag{3}$$

$$\delta = 12.5\frac{\left(\gamma/c\right)^{0.05}\left(\beta_1 + \beta_{2m}\right)^{0.63}\cos^2(\gamma)\left(t_{\max}/c\right)^{0.29}}{\left(32.3 + 0.01\beta_{1m}^{2.07}\right)\tanh^{0.2}(\text{Re}/\,200000)} \tag{4}$$

Multi-Fidelity ACE Performance Simulation

A multi-fidelity ACE performance simulation model is established in this section by integrating the 1D front fan mean-line analysis model, 1D rear fan mean-line analysis model, and 1D LPT mean-line analysis model into the 0D ACE model with the iteratively-coupled method. The advantage of the iteratively-coupled method is that the data from the 0D ACE model to the 1D adaptive fan and the LPT model can be transferred in both directions, respectively, without changing the mathematical model and architecture of the 0D ACE model, compared with the fully-coupled method.

The 0D/1D iteratively-coupled simulation process is shown in Figure 5. First, the flight conditions and engine control schemes are set, and 0D ACE simulation is carried out with the Newton-Raphson iterative solver to obtain the components' boundary conditions. The boundary conditions of the front fan and rear fan include the inlet total pressure Ptin, inlet total temperature Ttin, low-pressure spool speed N, total pressure ratio PR, and guide vane angle variation dVG, and the boundary conditions of the LPT include fuel air ratio FAR, cooling parameters in addition to those of the adaptive fan. Then the 1D front fan, 1D rear fan, and 1D LPT mean-line analysis are conducted to obtain the 1D performance of each component. Based on the results of the 0D ACE model and 1D turbomachinery models, the residuals of each component's mass flow rate W and the isentropic efficiency η are generated. When the residuals do not satisfy the convergence criterion, a set of correction factors of W and η are calculated, which are used to update the scaling factors of the front fan, rear fan, and LPT generic characteristic maps in the 0D ACE model. The above process is repeated until all the W and η residuals satisfy the convergence criterion. To realize the automatic data transfer in the iteratively-coupled simulation, the 0D ACE model constantly calls the executable files of the 1D adaptive fan models and the m-file of the 1D LPT model.

The residual Res can be calculated from Equation (5), where the subscript 1D denotes the parameters calculated by the 1D turbomachinery models and 0D denotes the parameters calculated by the 0D ACE model. The convergence criterion is that the residuals of each parameter do not exceed 1×10^{-4}.

$$\text{Res} = \left|p_{1\text{D}} - p_{0\text{D}}\right| / p_{0\text{D}} \tag{5}$$

The scaling factors of the mass flow rate f_W and efficiency f_η are calculated by Equation (6), referring to the literature (Klein et al., 2017), where i and i-1 denote the parameters of the current iteration step and the previous iteration step, respectively, and δ denotes the relaxing factor, used to suppress the residuals oscillation. In this paper, δ is set to 0.5.

$$f_{W,i} = \left[\left(\frac{W_{1D}}{W_{0D}} - 1\right)\cdot\delta + 1\right]\cdot f_{W,i-1}$$
$$f_{\eta,i} = \left[\left(\frac{\eta_{1D}}{\eta_{0D}} - 1\right)\cdot\delta + 1\right]\cdot f_{\eta,i-1} \quad (6)$$

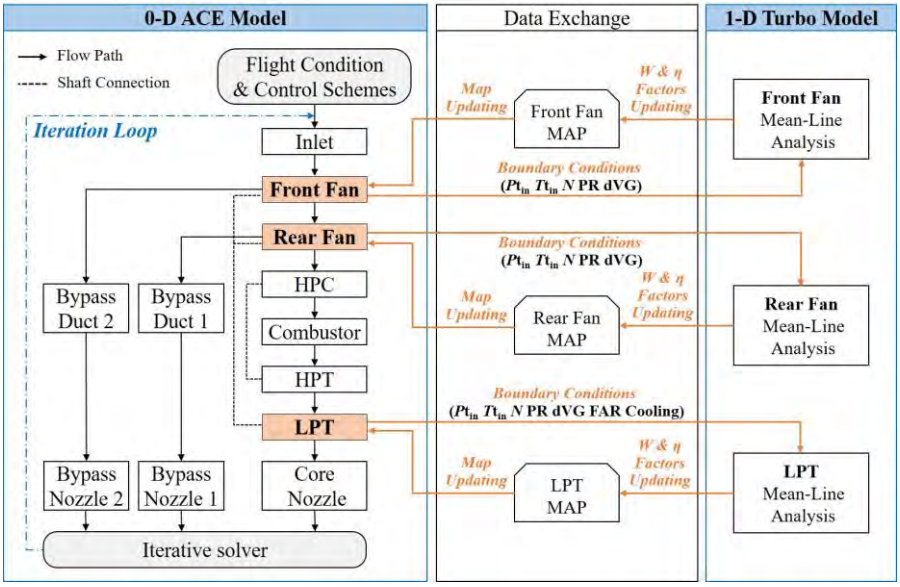

Figure 5 0D/1D Iteratively-Coupled Simulation Flow Chart

RESULTS AND DISCUSSION

Effect of component zooming on engine performance and computing time

The developed multi-fidelity ACE simulation approach enables free switching of the component dimension between 0D and 1D, realizing the component zooming function.

The performance comparisons of the multi-fidelity ACE models with different component zooming strategies are shown in Figure 6.

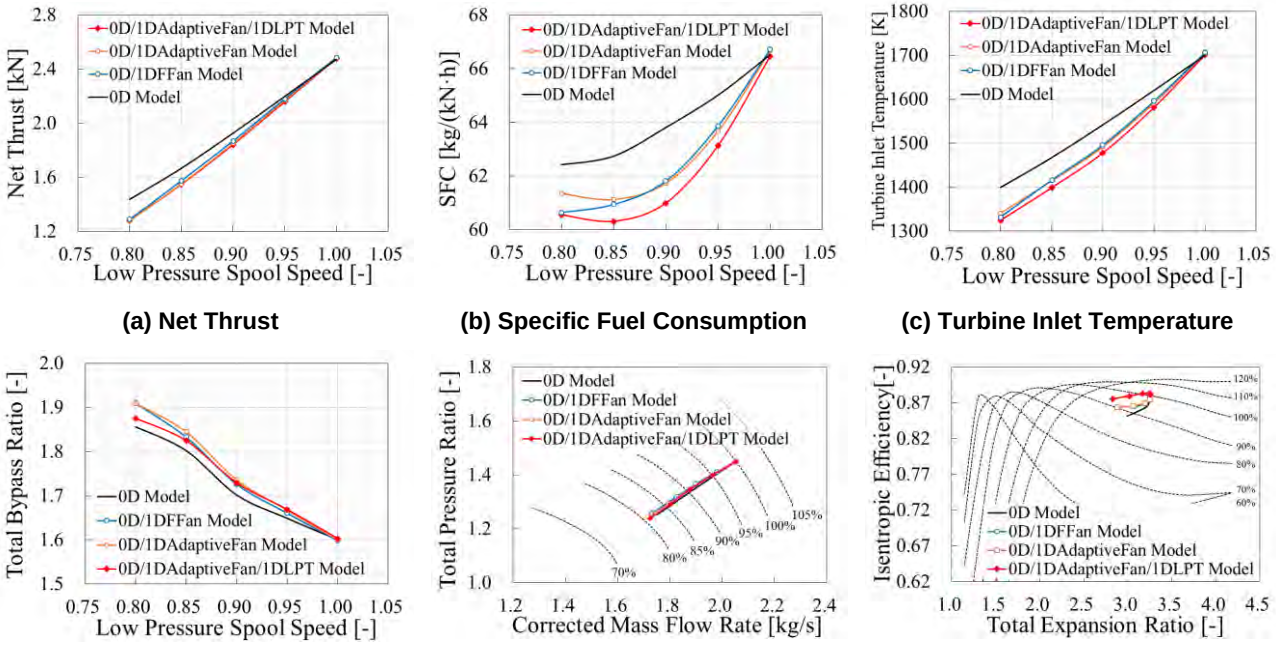

(a) Net Thrust **(b) Specific Fuel Consumption** **(c) Turbine Inlet Temperature**

(d) Total Bypass Ratio **(e) Operating Line on RFAN Map** **(f) Operating Line on LPT Map**

Figure 6 Performance Comparisons of Multi-Fidelity ACE Models

The legend *0D/1DFFan Model* denotes the results of coupling the 1D front fan model with the 0D ACE model, the legend *0D/1DAdaptiveFan Model* denotes the results of coupling the 1D front fan and 1D rear fan model with the 0D ACE model, and the legend *0D/1DAdaptiveFan/1DLPT Model* denotes the results of coupling the 1D adaptive fan and 1D LPT model with the 0D ACE model. RFAN denotes the rear fan. When the low-pressure spool speed is lower than 90% speed, the throat area of the second bypass nozzle increases by 8% to increase the front fan surge margin. As shown in Figure 6, the performance of the multi-fidelity models and 0D model at 100% low-pressure spool speed is basically the same, but the performance deviations increase as the speed decreases. Among all the multi-fidelity models, the 0D/1DAdaptiveFan/1DLPT model deviates the most from the 0D model regarding thrust, SFC, and T4. Compared with the multi-fidelity models, the 0D model overestimates the thrust, SFC, and T4, but underestimates the bypass ratio. The maximum deviations of thrust, SFC, T4, and bypass ratio between the 0D/1DAdaptiveFan/1DLPT model and 0D model are -10.8%, -4.4%, -5.4% (-75K), and 1.6%, respectively, which are considerable and non-negligible for the application in the design stage of ACE.

The computing time comparisons of different multi-fidelity ACE models at 100% and 90% low-pressure spool speeds are shown in Figure 7. FFAN denotes the front fan. The computing time of the 0D model is about 1.5 seconds. Due to the adoption of the 1D turbomachinery models and iteratively-coupled simulation, the computing time of the multi-fidelity models increases obviously. As the speed decreases, the component characteristic differences between the multi-fidelity models and the 0D model increase. Therefore more iterations are required, resulting in more computing time for off-design speed than for design speed. However, the computing time of this magnitude is short enough and quite acceptable to be applied in the preliminary design stage, compared to that of the massively parallel computation of the three-dimensional computational fluid dynamics (CFD) simulation. The computing time of all the multi-fidelity models is less than 2 minutes, and the main time spent comes from calling and running the 1D LPT model, which will be optimized to further reduce the computing time.

The variations of the residuals with the number of iterations at 90% low-pressure spool speed are shown in Figure 8. After 13 iterations, all the residuals meet the convergence criterion.

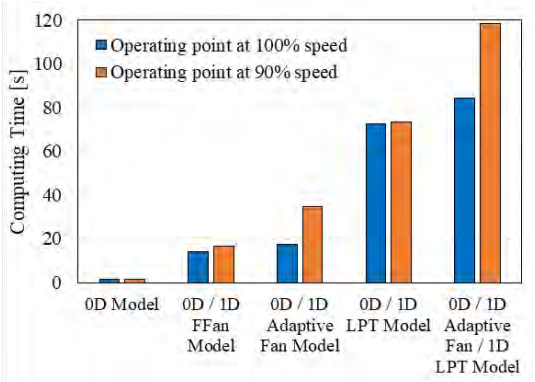

Figure 7 Computing Time Comparisons of Multi-Fidelity ACE Models

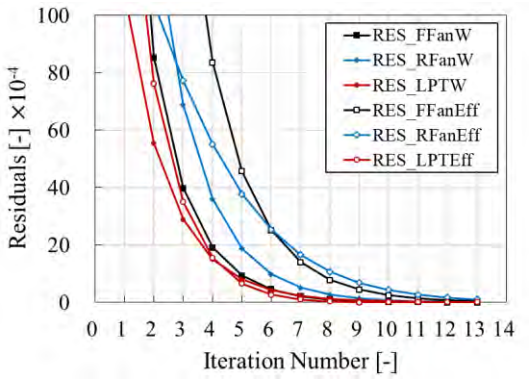

Figure 8 Variations of Residuals with Iterations

Effect of variable guide vane angle on engine performance

With the multi-fidelity models, the effect of variable guide vane angle on the engine performance can be evaluated. The 0D/1DAdaptiveFan/1DLPT model, abbreviated as the MD model, will be used for performance analysis in this and subsequent sections.

The effect of the rear fan inlet guide vane (IGV) angle on the engine performance at 100% low-pressure spool speed is shown in Figure 9, and the deviations between the MD model and 0D model are also presented. The negative angle indicates that the IGV is opened. As the rear fan IGV angle decreases from 0°, the rear fan mass flow rate and pressure ratio increase, leading to the increment of the rear fan power. The fuel consumption needs to be increased to keep the low-pressure spool operating at 100% speed, resulting in the increased T4 and thrust. As shown in Figure 9, the thrust, SFC, and T4 predicted by the 0D model are lower than those of the MD model, and when the rear fan IGV angle is set to -12°, the deviations are 4.5%, 4.7%, and 4.9% (85K), respectively. The multi-fidelity simulation approach proposed in this paper can also evaluate the effect of the variable geometries of multiple IGVs and stators on engine performance.

The effect of the LPT IGV angle on the component and engine performance at 90% low-pressure spool speed is shown in Figure 10 and Table 3, respectively. The two-stage LPT is utilized to fulfill the design value of the LPT expansion ratio equal to 3.2. IGV1 means the first stage IGV, while IGV2 means the second stage IGV. Similar to the adaptive fan, the negative angle indicates that the IGV is opened. In Figure 10, the operating points when IGV1 = -4°, 0°, 4° are shown on the component maps. As the LPT IGV1 angle decreases, the LPT flow capacity increases, resulting in a decrement in the LPT expansion ratio and an increment of the HPT expansion ratio. As a result, the high-pressure spool speed increases, the

bypass ratio decreases, and the back pressure of the front fan and rear fan decrease, leading to the operating points moving away from the surge boundary. In Table 3, the decrement of the LPT IGV1 results in the increment of the thrust and SFC, while the LPT IGV2 shows little effect on the performance, indicating that the aerodynamic throat of the present LPT design locates at the first stage.

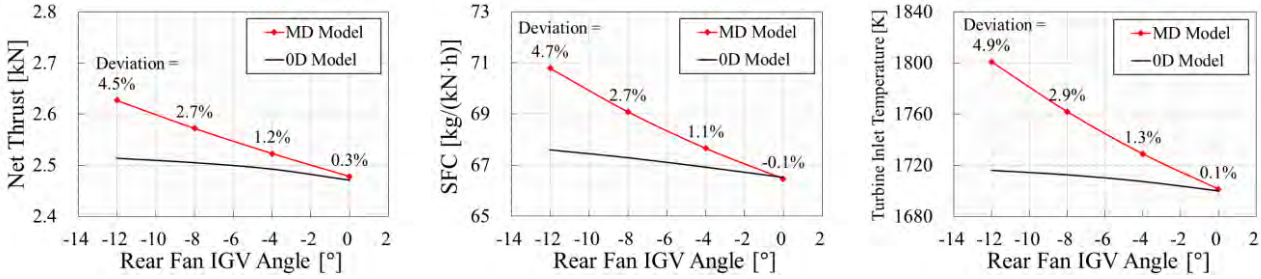

(a) Net Thrust **(b) Specific Fuel Consumption** **(c) Turbine Inlet Temperature**

Figure 9 Effect of Rear Fan IGV Angle on Engine Performance at 100% Low-pressure Spool Speed

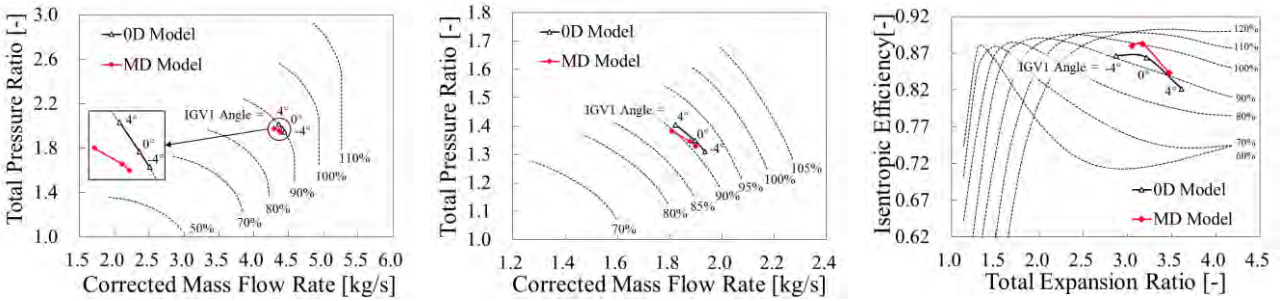

(a) Operating Point on FFAN Map **(b) Operating Point on RFAN Map** **(c) Operating Point on LPT Map**

Figure 10 Effect of LPT IGV1 Angle on Component Performance at 90% Low-pressure Spool Speed

Table 3 Effect of LPT IGV1 and IGV2 Angle on Engine Performance at 90% Low-pressure Spool Speed

IGV Angle dIGV [°]	Net Thrust [kN]	SFC [kg/(kN·h)]	T4 [K]	Bypass Ratio
dIGV1 = 0, dIGV2 = 0	1.841	60.99	1478	1.73
dIGV1 = -4, dIGV2 = 0	1.865	61.72	1483	1.66
dIGV1 = -4, dIGV2 = -2	1.867	61.79	1484	1.66
dIGV1 = -2, dIGV2 = -2	1.854	61.24	1477	1.68

To realize the switching of operating modes and the optimal performance in different modes, the ACEs require its components to have the capability of wide-range variable geometry, which brings a significant challenge for the ACE performance prediction with high accuracy. The multi-fidelity simulation approach proposed in this paper is a good tool to cope with the challenge above under the acceptable computing resources and time cost.

Effect of tip clearance on engine performance

Tip clearance is an intriguing and challenging topic in the development of aero-engines. Too large or small tip clearance will significantly affect the engine performance and operation safety. With the MD model, the effect of tip clearance on the engine performance can be evaluated, which usually can not be appropriately considered in the 0D model.

The effect of the LPT tip clearance on the engine performance at 100% low-pressure spool speed is shown in Table 4. The performance prediction model with changed tip clearance adopted here is from the literature (Agromayor and Nord, 2019). Because the engine mass flow rate is quite low, the ratio of tip clearance to blade height is large, resulting in a significant effect of the tip clearance on the LPT efficiency. The increase in the tip clearance leads to a decrease in the LPT efficiency and an increase in the SFC and T4. As the tip clearance increases, the performance deteriorations tend to slow down.

Table 4 Effect of LPT Tip Clearance on Engine Performance at 100% Low-pressure Spool Speed

Tip Clearance [mm]	Net Thrust [kN]	SFC [kg/(kN·h)]	T4 [K]	LPT Efficiency [-]
0	2.466	65.86	1689	0.892
0.2 (≈1% blade height)	2.478	66.46	1701	0.882
0.4 (≈2% blade height)	2.487	66.91	1711	0.875

0.6 (≈3% blade height)	2.494	67.32	1719	0.868
0.8 (≈4% blade height)	2.502	67.69	1727	0.863

CONCLUSIONS

In this paper, the integration of the 1D adaptive fan model and 1D LPT model into the 0D three-stream configuration ACE model is carried out for multi-fidelity ACE performance prediction, and the conclusions are drawn as follows:

1) An 0D/1D iteratively-coupled multi-fidelity simulation approach is proposed. In the proposed approach, the 1D front fan and rear fan mean-line analysis model packaged into executable files, and the 1D LPT mean-line analysis model written in m-files, are called by the 0D ACE model, respectively. The data transmission between the 0D ACE model and the 1D component model can be realized in both directions, without changing the mathematical model and architecture of the origin 0D ACE model. Furthermore, the proposed approach enables free switching of the adaptive fan and LPT model fidelity between 0D and 1D.

2) The performance parameters predicted by the multi-fidelity ACE models with different component zooming strategies are compared. The maximum deviations of thrust, SFC, T4, and bypass ratio between the 0D/1D Adaptive Fan/1D LPT coupled model and 0D ACE model are -10.8%, -4.4%, -75K, and 1.6%, respectively, which are considerable and non-negligible for the application in the design stage of ACE. In addition, the computing time of all the multi-fidelity models is less than 2 minutes, which can be further reduced by optimizing the coupled method and accelerating the component models' computation speed.

3) Taking the variable guide vane angle and tip clearance as examples, the effects of the key aerodynamic parameters of the adaptive fan and LPT on the performance are evaluated. The proposed approach has the ability to analyze the effects of the variable geometries of multiple IGVs/stators and tip clearance in detail according to the research needs, which usually can not be appropriately considered in the 0D ACE model.

4) The proposed approach provides a generic and efficient solution for multi-fidelity ACE performance prediction with acceptable computing resources and time cost, which is applicable in the engine conceptual and preliminary design stage.

Future works will focus on improving the multi-fidelity simulation approach, including increasing the accuracy and reducing the computing time, applying the approach to the multi-objective optimization of the engine performance and control schemes, and extending it to other components and other engine configurations. Particularly, we will further validate the multi-fidelity simulation approach in two ways. One is the application of the multi-fidelity approach in a simpler configuration engine with available characteristics and geometric information, the other is the establishment of the three-dimensional (3D) simulation model of the entire ACE for validation.

NOMENCLATURE

ACE	Adaptive Cycle Engine	T-MATS	Toolbox for the Modeling and Analysis of Thermodynamic Systems
c	Chord Length	Tt	Total Temperature
CDFS	Core-Driven Fan Stage	T4	Turbine Inlet Temperature
dVG	Guide Vane Angle Variation	W	Mass Flow Rate
f	Scaling Factor	β	Flow Angle
FAR	Fuel Air Ratio	β_m	Metal Angle
FFAN	Front Fan	γ	Stagger Angle
HPC	High-Pressure Compressor	δ	Relaxing Factor, or Deviation Angle
HPT	High-Pressure Turbine	ε	Flow Turning Angle
i	Incidence Angle	η	Isentropic Efficiency
IGV	Inlet Guide Vane	ω	Profile Loss Coefficient
LPT	Low-Pressure Turbine	0D	Zero-dimensional
M	Mach Number	1D	One-dimensional
MD	Multi-Fidelity Model		
N	Low-Pressure Spool Speed		
PR	Total Pressure Ratio	**SUBSCRIPT**	
Pt	Total Pressure	in	Inlet
Re	Reynolds Number	max	Maximum
RFAN	Rear Fan	ref	Reference State
SFC	Specific Fuel Consumption	1	Blade Inlet
t	Blade Thickness	2	Blade Outlet

ACKNOWLEDGMENTS

This research was supported by the National Science and Technology Major Project (J2019-I-0021-0020) and the National Science and Technology Major Project (J2019-II-0020-0041).

REFERENCES

Agromayor, R., and Nord, L. O. (2019). Preliminary Design and Optimization of Axial Turbines Accounting for Diffuser Performance. International Journal of Turbomachinery Propulsion and Power, 4(3): 32.

Alexiou, A., Baalbergen, E. H., Kogenhop, O., Mathioudakis, K., and Arendsen, P. (2007). Advanced Capabilities for Gas Turbine Engine Performance Simulations. ASME Turbo Expo 2007, GT2007-27086, Vol. 4790, pp. 19-28.

Baotong, W., Zhaoyun, S., Wangzhi, Z., Heli, Y., Mengyang, W., Kai, Z., Xudong, F. and Xinqian, Z. (2022). Rapid Performance Prediction Model of Axial Turbine with Coupling One-Dimensional Inverse Design and Direct Analysis. Aerospace Science and Technology, 130: 107828.

Chapman, J. W., Lavelle, T. M., May, R. D., Litt, J. S., and Guo, T. H. (2014). Toolbox for the Modeling and Analysis of Thermodynamic Systems (T-MATS) User's Guide, NASA/TM-2014-216638, No. E-18833.

Claus, R. W., Evans, A. L., Lylte, J. K., and Nichols, L. D. (1991). Numerical Propulsion System Simulation. Computing Systems in Engineering, 2(4), pp. 357-364.

Connolly, J. W., Friedlander, D. J., and Kopasakis, G. (2014). Computational Fluid Dynamics Modeling of A Supersonic Nozzle and Integration into A Variable Cycle Engine Model. 50th AIAA/ASME/SAE/ASEE Joint Propulsion Conference, Paper No. AIAA 2014-3687, p. 3687.

Creveling, H. F. and Carmody, R. H. (1967). Computer Program for Calculating Off-Design Performance of Multistage Axial-Flow Compressors. NASA-Lewis Research Center, NASA CR-72427.

Edmunds, D. B. (1977). Multivariable Control for a Variable Area Turbine Engine. Aeronautical System Division, Report ASD-TR-77-59, pp.4-19.

Fu, S., Li, Z., Zhanxue, W., Zhifu, L., and Jingwei, S. (2021). Integration of High-Fidelity Model of Forward Variable Area Bypass Injector into Zero-Dimensional Variable Cycle Engine Model. Chinese Journal of Aeronautics, 34(8), 1-15.

GE Aerospace. (2023). XA100 Adaptive Cycle Engine. *GE Aerospace website*, [online]. Available at: https://www.geaerospace.com/propulsion/military/xa100 [Accessed 8 Aug. 2023].

Grönstedt, T. (2000). Development of Methods for Analysis and Optimization of Complex Jet Engine Systems. Ph.D. Charmers University of Technology.

Guy, N. (2021). How GE's Adaptive Engine Differs From Earlier Variable-Cycle Designs. *Aviation Week Network*, [online]. Available at: https://aviationweek.com/defense-space/aircraft-propulsion/how-ges-adaptive-engine-differs-earlier-variable-cycle-designs [Accessed 14 May 2021].

Johnson, J. (1995). Variable Cycle Engine Developments. Developments in High-Speed-Vehicle Propulsion Systems, 165.

Junqiang, Z., and Sjolander, S. A. (2005). Improved Profile Loss and Deviation Correlations for Axial-Turbine Blade Rows. ASME Turbo Expo 2005, GT2005-69077, Vol. 47306, pp. 783-792.

Kacker, S. C., and Okapuu, U. (1982). A Mean Line Prediction Method for Axial Flow Turbine Efficiency. Journal of Engineering for Power, 104: 111-119.

Kim, S., Kim, D., Son, C., Kim, K., Kim, M., and Min, S. (2015). A Full Engine Cycle Analysis of a Turbofan Engine for Optimum Scheduling of Variable Guide Vanes. Aerospace Science and Technology, 47, 21-30.

Klein, C., Reitenbach, S., Schoenweitz, D., and Wolters, F. (2017). A Fully Coupled Approach for the Integration of 3D-CFD Component Simulation in Overall Engine Performance Analysis. ASME Turbo Expo 2017, GT2017-63591, Vol. 50770, p. V001T01A014.

Kolias, I., Alexiou, A., Aretakis, N., and Mathioudakis, K. (2018). Direct Integration of Axial Turbomachinery Preliminary Aerodynamic Design Calculations in Engine Performance Component Models. ASME Turbo Expo 2018, GT2018-76494, Vol. 50985, p. V001T01A030

Kopasakis, G., Cheng, L., and Connolly, J. W. (2015). Stage-by-Stage and Parallel Flow Path Compressor Modeling for A Variable Cycle Engine. 51st AIAA/SAE/ASEE Joint Propulsion Conference, AIAA 2015-4143, p. 4143.

Pilet, J., Lecordix, J. L. C., Garcia-Rosa, N., Barenes, R., and Lavergne, G. R. (2011). Towards a Fully Coupled Component Zooming Approach in Engine Performance Simulation. ASME Turbo Expo 2011, GT2011-46320, Vol. 54617, pp. 287-299.

Sullivan, T., and Parker, D. E. (1979). Design Study and Performance Analysis of A High-Speed Multistage Variable-Geometry Fan for A Variable Cycle Engine. NASA-Lewis Research Center, NASA-CR-159545.

Xiaobo Z., Zhanxue, W., and Li, Z. (2023). An Integrated Modeling Approach for Variable Cycle Engine Performance Analysis. Journal of the Franklin Institute, Vol. 360, pp. 5549-5563.

Zhaoyun, S., Baotong, W., Tengbo, F., Xinqian, Z. and Xudong, F. (2022). Rapid Prediction Method of Compressor Characteristics with Coupling Direct and Inverse Problems. Journal of Aerospace Power, 37(3): 619-628.